1 ***Clostridioides difficile*** **PCR ribotype 151 is polyphyletic and includes pathogenic isolates from**

2 **cryptic clade C-II with mono-toxin pathogenicity loci that can escape routine diagnostics**

3

4 Quinten R. Ducarmon[a,b], Jan-Tom van der Bruggen[c], Céline Harmanus[a], Ingrid M.J.G. Sanders[a], Laura

5 G.M. Daenen[d], Ad C. Fluit[c], Rolf H.A.M. Vossen[e], Susan L. Kloet[e], Ed J. Kuijper[a,b,f], Wiep Klaas

6 Smits[a,b,g#]

7

8 [a]Department of Medical Microbiology, Leiden University Medical Center, Leiden, The Netherlands.

9 [b]Center for Microbiome Analyses and Therapeutics, Leiden University Medical Center, Leiden, The

10 Netherlands.

11 [c]Department of Medical Microbiology, University Medical Centre Utrecht, Utrecht, The Netherlands.

12 [d]Department of Haematology, University Medical Centre Utrecht, Utrecht, The Netherlands.

13 [e]Leiden Genome Technology Center, Leiden University Medical Center, Leiden, The Netherlands

14 [f]Center for Infectious Disease Control, National Institute for Public Health and the Environment,

15 Bilthoven, The Netherlands.

16 [g]Centre for Microbial Cell Biology, Leiden, The Netherlands.

17 [#]Address correspondence to w.k.smits@lumc.nl

18

ABSTRACT

We report a patient case with pseudomembranous colitis associated with a mono-toxin producing *Clostridioides difficile* belonging to the very rarely diagnosed PCR ribotype (RT) 151. The infection was difficult to diagnose, since the isolate and the feces sample tested negative for toxin-encoding genes using a routine commercial test. This prompted us to sequence n = 11 RT151s from various geographical regions to study their genomic characteristics and relatedness. By including whole genome sequence data from other sources, we could further place these isolates into the phylogenetic tree of *C. difficile* and assign them to their respective clades. These analyses revealed that 1) RT151s are polyphyletic with isolates falling into clades 1, and cryptic clades C- I and C- II 2) RT151 contains both non-toxigenic and toxigenic isolates and 3) RT151 C-II isolates contained mono-toxin pathogenicity loci (PaLoc). Additional analysis with PacBio circular consensus sequencing revealed that the isolate from our patient case report contains a novel PaLoc insertion site, lacked *tcdA* and a had significantly divergent *tcdB* sequence that might explain the failure of the diagnostic test. The study is noteworthy as 1) RT151 encompasses both typical and cryptic clades and 2) conclusive evidence for CDI due to clade C-II isolates was hitherto lacking.

KEYWORDS: *Clostridioides difficile*, cryptic clade, PaLoc

36 **INTRODUCTION**

37 *Clostridioides difficile* is a Gram-positive, spore-forming anaerobic bacterium and the leading cause
38 of antibiotic-associated diarrhea, both in healthcare facilities and the community[1]. *C. difficile* can
39 produce several clostridial toxins (toxin A or TcdA, toxin B or TcdB and the binary toxin CDT) and
40 these are responsible for *C. difficile* infection (CDI), symptoms of which can range from mild and self-
41 limiting diarrhea to pseudomembranous colitis, toxic megacolon and ultimately death[1]. Phylogenetic
42 analyses have revealed that most *C. difficile* isolates associated with human and animal disease fall
43 within 5 clades[2]. In recent years, reports have appeared on (mainly environmental) isolates that are
44 phylogenetically distinct from these 5 clades, but rather fall within at least 3 so-called cryptic clades
45 (C-I, C-II and C-III) that can be considered a separate genomospecies[2-5]. Though cryptic clade isolates
46 can contain toxin genes[2, 4, 6], knowledge about the occurrence and clinical significance of these
47 isolates is limited.

48 Within clades 1-5, the pathogenicity locus harboring the the *tcdA* and/or *tcdB* genes is
49 generally located at a consistent location in the *C. difficile* genome (*cdu1*/*cdd1*) and further includes
50 several other accessory genes (*tcdR*, *tcdC* and *tcdE*) (Figure 1A and B)[6, 7]. Importantly, isolates
51 belonging to the cryptic clades C-I and C-III can have divergent pathogenicity locus (PaLoc)
52 sequences and atypical PaLoc insertion sites that can impact diagnostic tests[2, 4, 6, 8].

53 Here, we report a case of human CDI caused by a RT151 clade C-II isolate for which initial
54 diagnostic tests using Cepheid Xpert *C. difficile* BT assay were negative, even though *C. difficile* could
55 be cultured from patient feces and clinical symptoms corresponded to a CDI case. We show that the
56 cryptic C-II isolate cultured from this patient contains a mono-toxin B PaLoc at a novel location, and
57 that other RT151 isolates fall in phylogenetically divergent clades 1, C-I and C-II.

58

59 **MATERIALS AND METHODS**

60 ***Clostridioides difficile* culturing, ribotyping and toxin testing**

61 RT151 isolates analysed as part of this study were derived from various national and international
62 studies in which the Dutch National Expertise Center for *C. difficile* at Leiden University Medical
63 Center (LUMC) participated and had isolates available. The isolates originate from Greece, Malta,
64 The Netherlands and Spain between 2011 and 2021. Detailed information on all RT151 isolates,
65 including relevant accession numbers, is provided in Supplemental Table S1.

66 Isolates were cultured on TSS plates (Tryptic Soy Agar with 5% sheep blood, bioMérieux, The
67 Netherlands) or CLO plates (selective *C. difficile* medium containing cefoxitin, amphotericin B and
68 cycloserine, bioMérieux, The Netherlands). Capillary electrophoresis PCR ribotyping was performed
69 at the Dutch Expertise Centre for *C. difficile*, according to standard procedures[9]. Feces samples and
70 *C. difficile* isolates were analyzed by the Xpert *C. difficile* BT assay (Cepheid), that targets *tcdB*, *cdtA*
71 and a variant *tcdC* gene associated with epidemic strains, according to the manufacturer's
72 instructions. They were further characterized using an in-house multiplex PCR targeting the 16S
73 rRNA gene, *gluD*, and the genes encoding the large clostridial toxins and binary toxin[10] or a PCR
74 targeting *tcdB* alone[11]. Toxin status was additionally assessed using a toxin neutralization assay using
75 0.4 µM filter-sterilized culture supernatant from a 48-h culture in Brain-Heart Infusion (BHI) broth on
76 VeroE6 cells, using purified toxins (Sigma) and neutralizing anti-TcdA/B antitoxin (Techlab) as
77 controls[12]. Supernatants from 48-h BHI cultures were also analyzed using the VIDAS® *C. difficile* Toxin
78 A & B (Biomérieux), according to the manufacturer's instructions.

79

80 **DNA extraction and whole-genome sequencing**

81 A pure culture from a TSS plate was resuspended in phosphate-buffered saline (Media Products
82 Groningen) to 3 McFarland, and 24 µl of lysozyme (50 g L^{-1}) was added to 800 µl of this suspension.

83 The solution was incubated for 20 min at 37°C and 15 µl of proteinase K (20 g L^{-1}l; Roche) was added,
84 followed by a 20 min incubation at 37°C. DNA was extracted on the QiaSymphony platform (Qiagen,
85 The Netherlands), using the Qiasymphony Virus/Pathogen Midi Kit according to the manufacturer's
86 instructions. Isolated total DNA was submitted for sequencing to Genomescan (Leiden, The
87 Netherlands) on the Illumina Novaseq6000 platform with read length 150 bp in paired-end mode.

88 To generate complete genomes, three isolates (LUMCMM21 0001/0003, LUMCMM19 2333
89 and LUMCMM16 0013) were submitted for long read sequencing on the Pacific Biosciences (PacBio)
90 Sequel platform at the Leiden Genome Technology Center. To prepare high molecular weight total
91 DNA, isolates were cultured overnight in 10 mL BHI at 37°C. Cells from 5 mL of culture were pelleted
92 and processed using the Qiagen Genomic-tip 100/G, according to the manufacturer's instructions.
93 PacBio sequencing libraries were generated as follows. Genomic DNA was sheared with the
94 Megaruptor 3 system (Diagenode) using 35-40 cycles. SMRTbell® libraries were generated according
95 to the following manufacturer's procedure & checklist: Preparing whole genome and metagenome
96 libraries using SMRTbell® prep kit 3.0, PN 102-166-600 APR2022. To retain DNA corresponding to
97 plasmids <10 kb, no size-selection was applied. The libraries were sequenced on a PacBio Sequel II
98 platform with a 30 h movie time using Binding Kit v2.2, Sequencing Primer v5 and Sequencing Kit
99 v2.0.

100

101 ***C. difficile* genome retrieval**

102 Four additional RT151 genome sequences were obtained from the laboratory collection of the UK
103 Anaerobic Reference Unit (Supplemental Table S1); these were processed and sequenced previously
104 as part of their routine surveillance and typing activities but raw Illumina reads were processed in
105 parallel with the other RT151 genomes reported here for the purpose of this study, as described
106 below.

107 To assess the phylogenetic relationship of the eleven RT151 in the context of the previously
108 established clades of *C. difficile*, we downloaded additional isolate sequence data: we included two
109 isolates of each of the three cryptic clades (C-I, C-II and C-III)[2], 4 isolates of clade 1 (as this is the
110 largest group) and two isolates of clade 2-5 from the Leiden-Leeds collection[13, 14] (Supplemental
111 Table S1).

112

113 **Data processing, assembly and quality control**

114 Raw Illumina sequence data was cleaned and trimmed using fastp (v0.23.2)[15] and sequence quality
115 was inspected using Fastqc (v0.11.9) and Multiqc (v1.8)[16, 17]. Cleaned reads were assembled by using
116 SKESA (v2.4.0) and SPAdes (v3.15.3) with "–untrusted-contigs" and "–isolate" parameters[18, 19]. Only
117 contigs with length 500 >= bp were kept. Assembly quality and general characteristics of the
118 assemblies were assessed using QUAST (v5.0.2)[20]. The scaffolds obtained from SPAdes were used for
119 downstream analyses. Default parameters were used unless stated otherwise.

120 Raw PacBio sequence data from LUMCMM16 0013 (RT151, clade C-I), LUMCMM21 0001
121 (RT151, clade C-II) and LUMCMM19 2333 (RT151, clade C-II) was assembled using Flye (v2.9)[21]" and
122 the start position was fixed using Circlator and the "fixstart" parameter[22]. Assembly quality was
123 subsequently inspected using available output metrics from Flye, QUAST and completeness using
124 BUSCO (v5.3.2, dataset clostridia_odb10 creation date 2020-03-06)[23]. Analysis of m4C and m6A
125 methylation was performed using PacBio SMRT® Link Software (v11.0.0.146107).

126

127 ***C. difficile* genome annotations and sequence typing**

128 Prokka (v1.14.6) was used for rapid genome annotation and to obtain protein sequences, with the "–
129 kingdom Bacteria", "--genus Clostridioides" and "–species difficile" parameters[24]. For pan-genome

130 and core-genome analyses, Roary (v3.13.0) was ran on the PROKKA-annotated scaffolds with the "-e
131 mafft" parameters[25, 26].

132 The accessory genome was subsequently visualized in R (v4.2.0) using the ComplexHeatmap
133 package (v2.12.0)[27]. To construct a phylogenetic tree based on the core genes as identified by Roary,
134 we used IQTree (v2.2.0) with the "-B 2500" and "-m MFP" parameters for 2500 bootstrap replicates
135 and automated model selection[28, 29]. The best model was chosen based on the minimized BIC score
136 and was identified to be UNREST+F0+I+G4. The obtained phylogenetic tree was subsequently
137 visualized using iTOL v6 and the tree was rooted at midpoint[30].

138 Multi-locus sequence typing (MLST) was performed using mlst (v2.19.0) with the PubMLST *C.*
139 *difficile* database updated to October 21st 2021[31]. To assign clades to each of our sequence types, we
140 used the information contained in Knight et al, which includes a clade assignment for sequence
141 types[2]. Novel loci (sodA-116, recA-82 and glyA-140) were identified and their respective sequences
142 obtained by mlst using the "-q –novel parameters" and submitted to the pubmlst database. Based
143 on this, three isolates were assigned new sequence types (ST946, ST947 and ST948) through
144 PubMLST (https://pubmlst.org/).

145 Available metadata for all isolates, including newly assigned sequence types, are listed in
146 Supplemental Table 1.

147

148 **Data availability**

149 Raw sequence data is available at the European Nucleotide Archive under BioProject PRJEB52887.
150 Associated metadata can be found in Supplemental Table S1. All bioinformatic tools used for the
151 analyses are freely available through the references provided. Complete chromosomes for PacBio-
152 sequenced isolates can be found as accession numbers GCA_945861085 (LUMCMM21 0003),
153 GCA_945909465 (LUMCMM19 2333) and GCA_945909635 (LUMCMM16 0013). For PaLoc alignment

154 and insertion analyses, the corresponding regions were extracted from the complete genome

155 sequence of the reference strain *C. difficile* 630 (AM180355)[32]. The pHSJD-312 sequence was

156 obtained from accession MG973074[4]. The patient provided written informed consent.

157

158 **RESULTS AND DISCUSSION**

159 **Case description and identification of a RT151 isolate from a CDI patient**

160 In 2021, a 46-year-old female patient was diagnosed with acute myeloid leukemia and treated with
161 two courses of induction chemotherapy followed by allogeneic hematopoietic stem cell
162 transplantation (allo-HSCT) at the University Medical Center Utrecht (UMCU), a tertiary care center
163 in the Netherlands. Due to primary graft failure, the patient received a second allo-HSCT two months
164 later. Between the first allo-HSCT and engraftment after the second allo-HSCT, the patient was
165 neutropenic for a prolonged time. This period was complicated by candidemia with *Candida kefyr*,
166 treated with anidulafungin followed by fluconazole, two bacteraemia episodes with a multidrug
167 resistant *Klebsiella pneumoniae* treated with imipenem/cilistatin and probable pulmonary
168 aspergillosis for which the patient received antifungal treatment. The post-transplantation period
169 was complicated by early reactivation of cytomegalovirus treated with foscarnet and later letermovir
170 prophylaxis, and mild graft-versus-host disease of the skin for which the patient received topical
171 steroids.

172 In the week prior to the second allo-HSCT, the patient developed diarrhea (day 0) and feces
173 was positive for norovirus and sapovirus as tested by PCR. The commonly used molecular test for
174 *Clostridioides difficile* (Cepheid Xpert *C. difficile* BT) was negative on a stool sample at day 0. Despite
175 the use of loperamide, diarrhea persisted in the following weeks although subsequent PCRs for
176 noro- and sapovirus became negative. PCRs for rotavirus, enterovirus, *Salmonella*, *Shigella*, *Yersinia*,
177 *Campylobacter*, *Plesiomonas*, *Giardia, Cryptosporidium*, *Dientamoeba fragilis*, *Blastocystis hominis*,
178 *Entamoeba histolytica* were also negative. The Xpert *C. difficile* BT assay was repeatedly negative on
179 day 43, day 45 and day 49. Colon biopsies taken on day 53 showed no signs of graft-versus-host
180 disease or pseudomembranous colitis. Around day 50 to 55, diarrhea seemed to diminish, but
181 around day 65 it started to intensify with up to ten watery stools per day in the ensuing weeks.
182 Repeated stool tests for viral, bacterial and parasitic infection were negative, including microscopy

183 for helminth eggs, cysts and *Cyclospora* and the Xpert *C. difficile* BT (on day 66, day 80, day 84 and
184 day 86). However, macroscopic findings during colonoscopy performed on day 82 were suggestive of
185 pseudomembranous colitis, confirmed by microscopy of colon biopsies while there were no signs of
186 graft-versus-host disease. These findings prompted treatment with oral vancomycin starting on day
187 84 using a taper-and-pulse regimen. After 4-5 days, the patient started to improve considerably with
188 stools becoming less frequent, lower stool volumes and a more solid consistency. Ethanol-treated
189 fecal material obtained on day 84 was culture-positive for *C. difficile* on cycloserine cefetoxin
190 fructose agar after 48h anaerobic incubation, as confirmed by matrix-assisted laser
191 desorption/ionization time-of-flight mass spectrometry. On day 159 (35 days after completion of
192 anti-CDI treatment), the patient developed a mild episode of diarrhea with abdominal cramps at
193 home, with negative Xpert *C. difficile* BT test on stool but again a positive culture of *C. difficile* from
194 feces that was later confirmed to belong to RT151. The patient spontaneously recovered without
195 antibiotic treatment within the two weeks that followed. Both isolates tested negative in the Xpert
196 *C. difficile* BT assay, but positive when using an in–house developed PCR for *C. difficile* toxin B[11]. Both
197 isolates were then sent to the Dutch Expertise Centre for *C. difficile* at the LUMC, with the first
198 isolate receiving the identification number LUMCMM21 0001 and the second isolate LUMCMM21
199 0003. Both isolates were characterized by capillary PCR ribotyping as RT151.
200
201 **RT151 isolates have different toxin profiles**

202 To obtain a better insight into the prevalence and characteristics of RT151, we retrieved all isolates
203 from the collection of the Dutch Expertise Center for *C. difficile*, that encompasses > 22000 isolates
204 collected since 2005. Seven isolates had been typed as RT151 using either agarose-gel based
205 ribotyping or capillary electrophoresis-based PCR ribotyping, demonstrating that this is a very rarely
206 diagnosed PCR ribotype (<0.035%).

207 Within this collection of RT151 isolates, five were non-toxigenic *C. difficile* (NTCD) and two
208 were toxigenic on the basis of a multiplex PCR. The isolate obtained from the case description from
209 Utrecht (LUMCMM21 0001) was positive for the gene encoding toxin B, but not the gene encoding
210 toxin A (A^-B^+), while an isolate obtained from a patient in Malta in 2019 (LUMCMM19 2333) had a
211 mono-toxin A (A^+B^-) and neither isolate contained the binary toxin locus according to PCR results.

212 These results are in line with findings of the Leeds Teaching Hospitals NHS Trust and
213 University of Leeds that report a prevalence for RT151 of <0.03% with varying toxin status in a cell
214 cytotoxicity and neutralization assay (CCNA; personal communication K.A. Davies and J. Freeman).

215 We also assessed toxigenicity using a diagnostic enzyme-linked fluorescent assay (VIDAS®,
216 bioMérieux) and a VeroC6-based CCNA. The result showed that only the *tcdB*-positive LUMCMM21
217 0001/0003 tested positive for toxin production (Supplemental Table S1). No toxin production could
218 be demonstrated for the *tcdA*-containing isolate (LUMCMM19 2333) under the conditions tested.

219

220 **Core genome phylogeny places some RT151 isolates in cryptic clade C-I and C-II**

221 To determine the relatedness between our RT151 isolates and to understand their placement in the
222 phylogenetic tree of *C. difficile*, we performed Illumina short-read whole genome sequencing (WGS).
223 In addition to the seven RT151 isolates obtained from our in-house collection, the UK Anaerobic
224 Reference Unit provided WGS data from four additional RT151 isolates. From a detailed analysis it
225 became clear that the two isolates isolated from the patient described above (LUMCMM21 0001 and
226 LUMCMM21 0003) are identical (data not shown).

227 By placing the eleven RT151 isolates into a phylogenetic tree with representative isolates
228 from cryptic clades I - III clades and all 'traditional' clades to ensure genetic diversity in our tree, we
229 assigned the RT151 isolates to their respective clades based on 1158 core genes in our analysis
230 (Figure 1). This analysis revealed that the majority (n = 8) of our RT151 isolates belonged to Clade 1

231 and MLST typing revealed these to be ST205 (or highly related ST type(s); ST205-like) (Supplemental
232 Table 1 and Figure 1). All of the RT151 isolates obtained from the UK Anaerobic Reference Unit fell
233 into ST205 (or ST205-like) groups and were therefore not further analyzed. Interestingly, three of the
234 isolates were classified into cryptic clades, with two independent isolates belonging to clade C-II
235 (LUMCMM21 0001/0003 and LUMCMM19 2333) and one isolate to clade C-I (LUMCMM16 0013).

236 These data demonstrate that *C. difficile* ribotype 151 is polyphyletic with isolates from the
237 same ribotype falling into two different cryptic clades as well as a 'regular' clade, which has not been
238 reported before. Though there is good concordance between PCR ribotype and MLST-based
239 approaches[13, 33, 34], these findings underscore that PCR ribotyping is insufficiently discriminatory for
240 phylogenetic placement.

241

242 **A pan-genome analysis suggests that accessory genes are not limited to specific clades**

243 It is conceivable that despite divergent core genomes, RT151 share a common accessory genome.
244 Therefore, we next investigated the accessory genes. We identified a total of 14,297 accessory genes
245 and these were clustered using the complete linkage method with Euclidian distances in the
246 ComplexHeatmap package[27] to identify potential similarities in the accessory genome of RT151 or
247 ST205 (Figure 2). In contrast to the clear clustering of RT151/ST205 isolates based on core phylogeny
248 (Figure 1), we did not observe such a pattern based on the accessory genes (Figure 2). Even isolates
249 from the same clades have widely divergent accessory genomes, suggesting that, the accessory
250 genome is not conserved at the level of STs or even clades, consistent with an open pangenome[2].

251

252 **Cryptic clade C-II RT151 isolates can have a mono-toxin pathogenicity locus at a novel insertion**
253 **site**

254 On the basis of our initial Illumina-sequenced genomes we were unable to recover PaLoc sequences
255 on a single contig for all isolates and, importantly, genomic neighborhoods around the PaLoc could
256 not be fully resolved. In particular, for the *tcdB*-positive C-II isolate from the Netherlands
257 (LUMCMM21 0003), *tcdB* was contained on a 18-kb contig lacking flanking chromosomal regions.
258 Additionally, we noted limited homology to the pHSJD-312 plasmid (Supplemental Figure S1A),
259 which carries a similar PaLoc. However, in contrast to the PaLoc on this plasmid, the LUMCMM21
260 0003 PaLoc lacked the binary toxin genes, *cdtA* and *cdtB*.

261 To identify the PaLoc insertion site and to establish whether it is carried on plasmid, we
262 generated complete genomes for the three cryptic clade RT151 isolate using PacBio circular
263 consensus sequencing (Table 1). The non-toxigenic C-I isolate (LUMCMM16 0013) was found to
264 contain extrachromosomal elements (ECEs) of 132 kb and 60 kb, that are classified in a PHASTER
265 prediction as possible and putative phage, respectively. The *tcdB* positive C-II isolate (LUMCMM21
266 0003) showed only a single contig, demonstrating that the toxin gene is not carried on a plasmid.
267 The *tcdA*-positive C-II isolate (LUMCMM19 2333) harbors a 13-kb ECE plasmid but this plasmid does
268 not contain toxin genes. Thus, in contrast to previous reports from C-I strains[4, 8], the cryptic RT151
269 isolates appear to carry their toxins on the chromosome.

270 PacBio sequencing also allows us to identify motifs associated with m4C and m6A
271 methylation events (Supplemental Table S2). Methylation has been reported to affect virulence
272 characteristics of *C. difficile*[35]. Notably, all strains contain the CamA-dependent modification of
273 CAAAA**A** sequences (modified residue in bold)[35, 36], indicating that the action of this
274 methyltransferase is conserved in the RT151 C-I and C-II strains. We also observed m6A methylation
275 on a subset of CAAA**A**AASNV motifs in the C-II strains, but not the C-I strain, suggesting it may be
276 specific for clade C-II. Finally, we observed m4C modification on a subset of **C**TATTATCW motifs in
277 the C-II strains, that may be conserved in C-I strains (CWATTATCW). This motif has not previously
278 been identified by others[35].

279 Next, we investigated the genomic location of the PaLoc's of the RT151 isolates by aligning
280 the observed insertion sites to those known ones from literature (Figure 1A)[4, 6], using the genome
281 sequence of the RT012 reference strain 630 and the sequence of plasmid pHSJD-312as a reference
282 (Figure 3)[4, 32]. This analysis reveals that the PaLoc in the Dutch C-II isolate is inserted at a location
283 that has not previously been described, between genes homologous to *cd0628* and *cd0629* of strain
284 630 (Figure 3C).

285 The PaLoc of LUMCMM21 0003, as well as the *cdu1-cdd1* insertion site that normally
286 harbors the PaLoc, is reminiscent of what has been described for a toxin A-negative toxin B-positive
287 toxinotype XXXII strain, 173070[5]. Similar to our isolate, the *cdu1-cdd1* locus contains a multi-gene
288 insertion interrupted by an IS256 insertion element and the PaLoc has a *tcdR-tcdB-tcdE* architecture,
289 lacks the binary toxin genes but has a divergently transcribed transcriptional regulator gene
290 upstream from *tcdR* (presumably this is *cdtR*). Though strain 173070 was sequenced, the data is not
291 publicly available and we were therefore unable to establish that this strain is phylogenetically
292 related to LUMCMM21 0003. We do note however, that the SLO148 ribotype reported in the
293 manuscript[5] is highly similar to that of RT151 (data not shown) and the reported ST (ST200) is
294 classified as C-II in other studies[2, 37].

295 The PaLoc in the Maltese C-II isolate (LUMCMM19 2333) is inserted between *spoVAE* and
296 *cd0776*, as previously described for isolate RA09-70[6] (Figure 1A, Supplemental Figure S1). RA09-70
297 was classified as Clade 5 but the phylogenetic analysis by the authors of the manuscript included
298 only strains from clade 1-5 and C-I. We therefore cannot exclude the possibility that RA09-70 is, in
299 fact, a clade C-II isolate that was misclassified as clade 5 for lack of reference.

300

301 **The role of C-II isolates in CDI**

302 To the best of our knowledge, the present study is the first to conclusively link a clade C-II isolate to
303 human disease, although the above sentences indicate that clade C-II isolates could be more
304 common than hitherto assumed. Nevertheless, diagnosis of CDI due to LUMCMM21 0001/0003 was
305 hampered by the fact that fecal samples, as well as *C. difficile* isolates, tested negative in the Xpert *C.*
306 *difficile* BT assay, used by many laboratories worldwide. Toxin gene sequences of cryptic clade
307 isolates can differ significantly from those of regular clade 1-5 isolates which can lead to false
308 negative results[4, 5]. Due to the proprietary nature of the Xpert *C. difficile* BT assay, we could not
309 confirm that this failure is due to mismatches between the primers used in the assay and the C-II
310 *tcdB* sequence but we have informed the company and provided the WGS data to investigate this
311 further. We do note that positive identifications were made using the ECDC-endorsed multiplex PCR
312 (relating to little or no mismatches in the primer sequence compared to the genome). A recent
313 report investigating *C. difficile* isolates from environmental locations showed several atypical PaLoc
314 locations in cryptic clade isolates and *in silico* PCR further suggested that routine diagnostic assays
315 would return highly variable results if such isolates would be encountered in the clinic[3], which is in
316 line with what we found in the current study. This underscores the potential of these isolates to be
317 OneHealth pathogens. Toxin-based assays (CCNA and VIDAS®) demonstrated toxin production for
318 the mono-toxin B isolate (LUMCMM21 0001/0003), but not the mono-toxin A isolate (LUMCMM19
319 2333). Though the latter was isolated from a hospitalized patient, lack of metadata did not allow us
320 to establish whether the patient had symptoms consistent with CDI and it remains to be established
321 if this isolate is pathogenic. Recently, it has been reported that toxin A-positive toxin B-negative C-III
322 strains cannot be identified on ChromID agar due to their esculin-negative nature[38]. We found,
323 however, that all RT151 strains – including those belonging to clades C-I and C-II, were esculin-
324 positive (Supplemental Table S1).

325 Altogether, reports of cryptic clade isolates that cause human CDI are still very rare. With
326 the increasing rate of community-onset CDI[39] and the discovery that cryptic clade isolates with
327 atypical PaLoc configurations are widespread in the environment [3], it is very likely that other CDI

328 cases caused by isolates from this cryptic clade occur but are missed by standard diagnostics if only

329 PCR is used.

330

Acknowledgements

The authors thank K. Galea (L-Università ta' Malta); J. Freeman and K. Davies (University of Leeds) for sharing unpublished data; Michael Perry and Trefor Morris (Anaerobic Reference Unit, Cardiff) for providing RT151 whole genome sequence information; I. Sidorov for implementation of clinker; and members of the Experimental Bacteriology Group at the LUMC for helpful discussions.

Funding

No external funding was received for this study.

Conflict of interest

EJK holds an unrestricted research grant from Vedanta Biosciences. All other authors: none to declare.

Author contributions

QRD: software, validation, formal analysis, data curation, writing - original draft, visualisation; JTvdB: writing – original draft; CH: investigation ; IMJGS: investigation; LD: resources; ACF: investigation; RHAMV: investigation, formal analysis; SLK: resources, supervision; EJK: conceptualization, writing - original draft; WKS: conceptualization, formal analysis, writing - original draft, visualization, supervision. All authors reviewed and edited the manuscript, and approved the final version.

350 **LEGENDS**

351 **Figure 1. RT151 isolates are part of clade 1, cryptic clade C-I and C-II and belong to various**

352 **sequence types**. The tree was rooted at midpoint in iTOL version 6. Detailed information, including

353 the depicted classifications, are available in Supplemental Table S1.

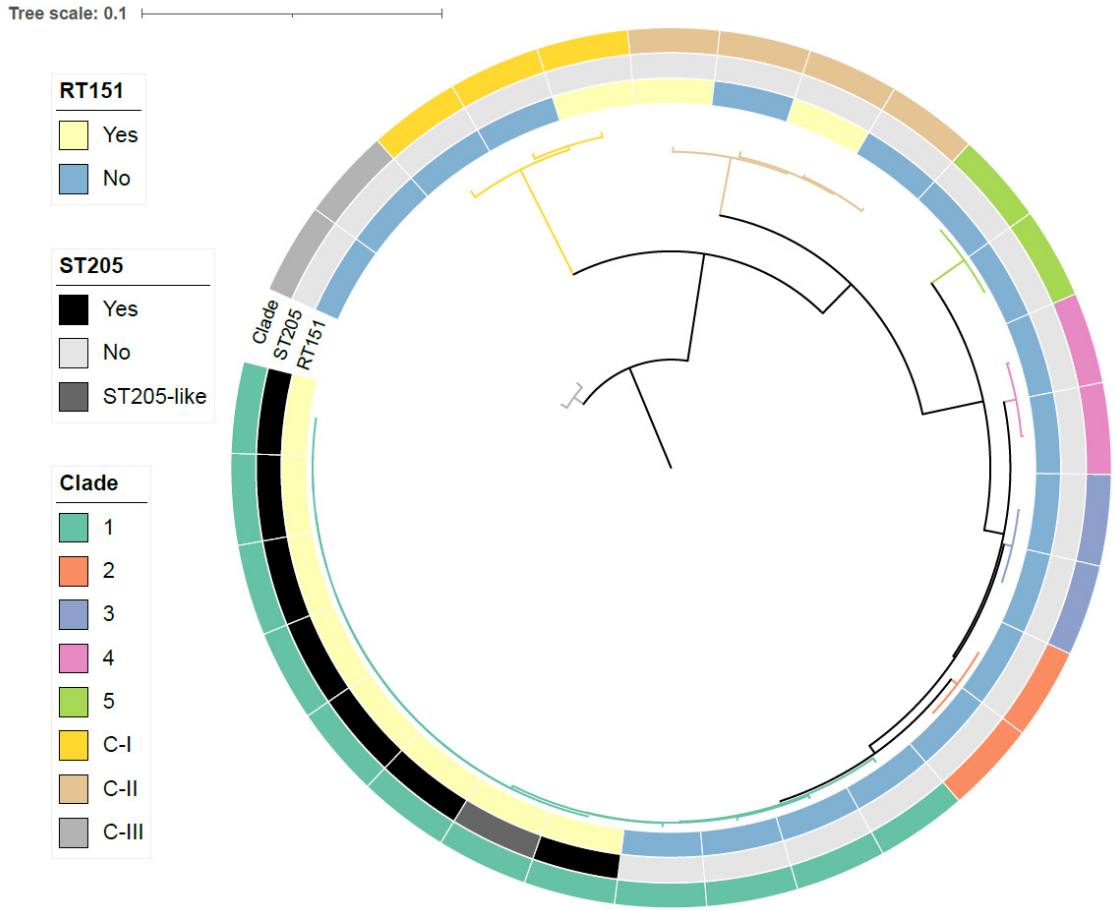

354

355

356

357 **Figure 2. No clustering of RT151 isolates based on the accessory genome (n = 14,297 genes).** Black
358 denotes the presence of a gene, white denotes the absence of a gene. Clustering of accessory genes
359 was performed using the complete linkage method with Euclidian distances in the ComplexHeatmap
360 package[27]. Detailed information, including the depicted classifications, are available in Supplemental
361 Table S1. Coloring is the same as in Figure 1.

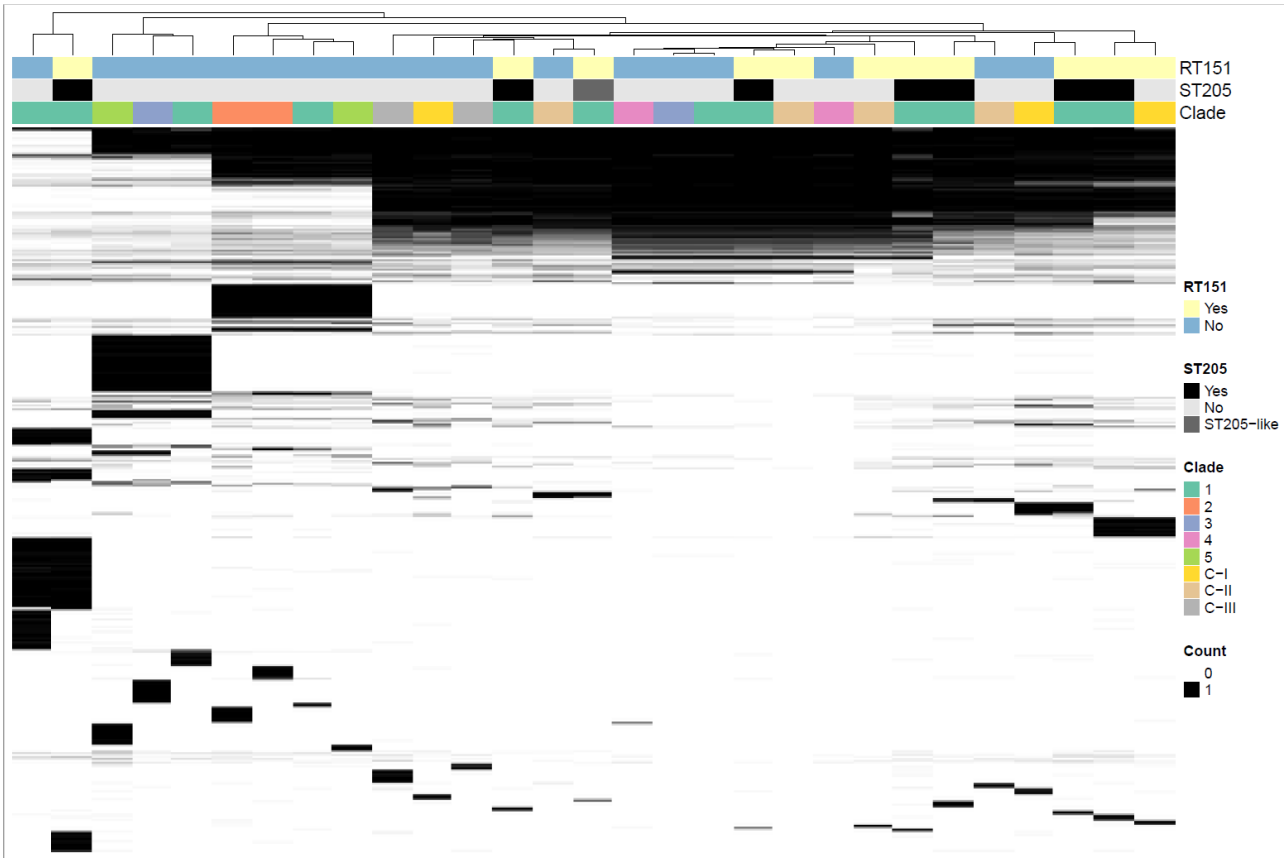

362

363

364 **Figure 3. Structure of the mono-toxin pathogenicity locus and PaLoc insertion sites of two cryptic**
365 **clade-II RT151 strains. A.** Overview of known PaLoc insertion sites (above the lines)[4, 6] and the novel
366 PaLoc insertion site (below the line) identified in the present study. Three sites are located on the
367 chromosome (nomenclature from RT012 reference strain 630)[32], and one is located on a plasmid
368 (nomenclature from clade C-I strain strain HSJD-312)[4, 8]. **B**. Structure of the PaLoc in the A-B+ RT151
369 clade C-II strain (LUMCMM21 0001/0003) showing all open reading frames predicted by Prokka[24].
370 Genes involved in transposition or recombination are indicated in red, hypothetical genes with
371 homology to the PaLoc on pHSJD-312 are indicated in gray, genes encoding toxin regulators are
372 indicated in green, the toxin gene is in orange and the holin gene in purple. **C**. Alignment of the
373 chromosomal region incorporating the *cd0628-cd0629* insertion site for RT151 isolates in
374 comparison with the RT012 reference strain 630[32]. RT151 clade 1 is LUMCMM11 0004, RT151 clade
375 C-I is LUMCMM16 0013, and RT151 clade C-II are LUMCMM21 0001/0003 (The Netherlands) and
376 LUMCMM19 2333 (Malta). Figure generated by clinker[40]and centered on *cd0628*. Colored arrows
377 indicate similar genes; links are drawn between similar genes on neighboring clusters and are
378 shaded based on sequence identity (0% white, 100% black, identity threshold for visualization 0.35).

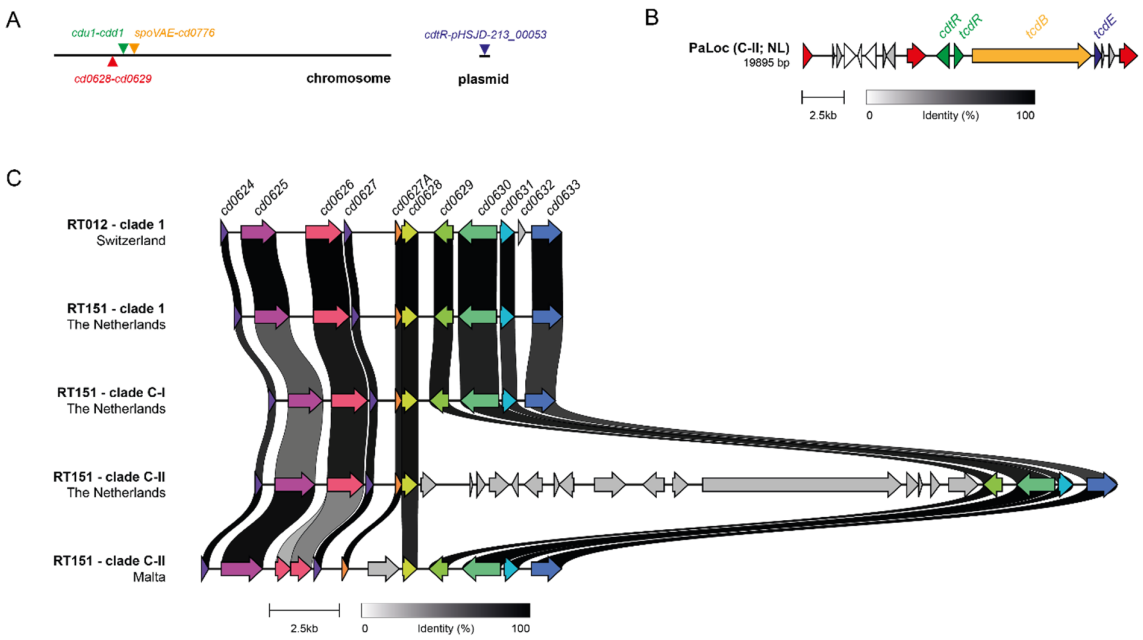

379

380 **Table 1. Genome characteristics of the cryptic clade RT151 isolates**

Isolate	Clade	Size (bp)	%GC	#ORFs	GenBank
LUMCMM16 0013	C-I	4169505 (chromosome) 132414 (possible phage) 59572 (putative phage)	28.8% 26.3% 26.6%	3747 174 79	GCA_945909635
LUMCMM21 0003	C-II	4108918 (chromosome)	28.7%	3688	GCA_945861085
LUMCMM19 2333	C-II	4424808 (chromosome) 12730 (putative plasmid)	28.7% 25.9%	4020 17	GCA_945909465

381

382 **REFERENCES**

383 1. Smits WK, Lyras D, Lacy DB, Wilcox MH, Kuijper EJ. Clostridium difficile infection. Nat Rev Dis
384 Primers. 2016;2:16020.
385 2. Knight DR, Imwattana K, Kullin B, Guerrero-Araya E, Paredes-Sabja D, et al. Major genetic
386 discontinuity and novel toxigenic species in Clostridioides difficile taxonomy. Elife. 2021;10.
387 3. Williamson CHD, Stone NE, Nunnally AE, Roe CC, Vazquez AJ, et al. Identification of novel,
388 cryptic Clostridioides species isolates from environmental samples collected from diverse
389 geographical locations. Microb Genom. 2022;8(2).
390 4. Ramírez-Vargas G, López-Ureña D, Badilla A, Orozco-Aguilar J, Murillo T, et al. Novel Clade C-I
391 Clostridium difficile strains escape diagnostic tests, differ in pathogenicity potential and carry toxins
392 on extrachromosomal elements. Sci Rep. 2018;8(1):13951.
393 5. Janezic S, Marín M, Martín A, Rupnik M. A new type of toxin A-negative, toxin B-positive
394 Clostridium difficile strain lacking a complete tcdA gene. J Clin Microbiol. 2015;53(2):692-5.
395 6. Monot M, Eckert C, Lemire A, Hamiot A, Dubois T, et al. Clostridium difficile: New Insights
396 into the Evolution of the Pathogenicity Locus. Sci Rep. 2015;5:15023.
397 7. Braun V, Hundsberger T, Leukel P, Sauerborn M, von Eichel-Streiber C. Definition of the
398 single integration site of the pathogenicity locus in Clostridium difficile. Gene. 1996;181(1-2):29-38.
399 8. Ramírez-Vargas G, Rodríguez C. Putative Conjugative Plasmids with tcdB and cdtAB Genes in
400 Clostridioides difficile. Emerg Infect Dis. 2020;26(9):2287-90.
401 9. Fawley WN, Knetsch CW, MacCannell DR, Harmanus C, Du T, et al. Development and
402 validation of an internationally-standardized, high-resolution capillary gel-based electrophoresis
403 PCR-ribotyping protocol for Clostridium difficile. PLoS One. 2015;10(2):e0118150.
404 10. ECDC. Laboratory procedures for diagnosis and typing of human *Clostridium difficile*
405 infection. Stockholm: ECDC; 2018.
406 11. Wolfhagen MJ, Fluit AC, Torensma R, Poppelier MJ, Verhoef J. Rapid detection of toxigenic
407 Clostridium difficile in fecal samples by magnetic immuno PCR assay. J Clin Microbiol.
408 1994;32(7):1629-33.
409 12. van den Berg RJ, Bruijnesteijn van Coppenraet LS, Gerritsen HJ, Endtz HP, van der Vorm ER,
410 et al. Prospective multicenter evaluation of a new immunoassay and real-time PCR for rapid
411 diagnosis of Clostridium difficile-associated diarrhea in hospitalized patients. J Clin Microbiol.
412 2005;43(10):5338-40.
413 13. Baktash A, Corver J, Harmanus C, Smits WK, Fawley W, et al. Comparison of Whole-Genome
414 Sequence-Based Methods and PCR Ribotyping for Subtyping of Clostridioides difficile. J Clin
415 Microbiol. 2022;60(2):e0173721.
416 14. Knetsch CW, Terveer EM, Lauber C, Gorbalenya AE, Harmanus C, et al. Comparative analysis
417 of an expanded Clostridium difficile reference strain collection reveals genetic diversity and
418 evolution through six lineages. Infect Genet Evol. 2012;12(7):1577-85.
419 15. Chen S, Zhou Y, Chen Y, Gu J. fastp: an ultra-fast all-in-one FASTQ preprocessor.
420 Bioinformatics. 2018;34(17):i884-i90.
421 16. Andrews S. FastQC: a quality control tool for high throughput sequence data. Babraham
422 Bioinformatics, Babraham Institute, Cambridge, United Kingdom; 2010.
423 17. Ewels P, Magnusson M, Lundin S, Käller M. MultiQC: summarize analysis results for multiple
424 tools and samples in a single report. Bioinformatics. 2016;32(19):3047-8.
425 18. Souvorov A, Agarwala R, Lipman DJ. SKESA: strategic k-mer extension for scrupulous
426 assemblies. Genome Biol. 2018;19(1):153.
427 19. Prjibelski A, Antipov D, Meleshko D, Lapidus A, Korobeynikov A. Using SPAdes De Novo
428 Assembler. Curr Protoc Bioinformatics. 2020;70(1):e102.
429 20. Gurevich A, Saveliev V, Vyahhi N, Tesler G. QUAST: quality assessment tool for genome
430 assemblies. Bioinformatics. 2013;29(8):1072-5.

431 21. Kolmogorov M, Yuan J, Lin Y, Pevzner PA. Assembly of long, error-prone reads using repeat
432 graphs. Nat Biotechnol. 2019;37(5):540-6.
433 22. Hunt M, Silva ND, Otto TD, Parkhill J, Keane JA, et al. Circlator: automated circularization of
434 genome assemblies using long sequencing reads. Genome Biol. 2015;16:294.
435 23. Manni M, Berkeley MR, Seppey M, Simão FA, Zdobnov EM. BUSCO Update: Novel and
436 Streamlined Workflows along with Broader and Deeper Phylogenetic Coverage for Scoring of
437 Eukaryotic, Prokaryotic, and Viral Genomes. Mol Biol Evol. 2021;38(10):4647-54.
438 24. Seemann T. Prokka: rapid prokaryotic genome annotation. Bioinformatics.
439 2014;30(14):2068-9.
440 25. Page AJ, Cummins CA, Hunt M, Wong VK, Reuter S, et al. Roary: rapid large-scale prokaryote
441 pan genome analysis. Bioinformatics. 2015;31(22):3691-3.
442 26. Katoh K, Misawa K, Kuma K, Miyata T. MAFFT: a novel method for rapid multiple sequence
443 alignment based on fast Fourier transform. Nucleic Acids Res. 2002;30(14):3059-66.
444 27. Gu Z, Eils R, Schlesner M. Complex heatmaps reveal patterns and correlations in
445 multidimensional genomic data. Bioinformatics. 2016;32(18):2847-9.
446 28. Hoang DT, Chernomor O, von Haeseler A, Minh BQ, Vinh LS. UFBoot2: Improving the
447 Ultrafast Bootstrap Approximation. Mol Biol Evol. 2018;35(2):518-22.
448 29. Minh BQ, Schmidt HA, Chernomor O, Schrempf D, Woodhams MD, et al. IQ-TREE 2: New
449 Models and Efficient Methods for Phylogenetic Inference in the Genomic Era. Mol Biol Evol.
450 2020;37(5):1530-4.
451 30. Letunic I, Bork P. Interactive Tree Of Life (iTOL) v5: an online tool for phylogenetic tree
452 display and annotation. Nucleic Acids Res. 2021;49(W1):W293-w6.
453 31. Jolley KA, Bray JE, Maiden MCJ. Open-access bacterial population genomics: BIGSdb
454 software, the PubMLST.org website and their applications. Wellcome Open Res. 2018;3:124.
455 32. Sebaihia M, Wren BW, Mullany P, Fairweather NF, Minton N, et al. The multidrug-resistant
456 human pathogen Clostridium difficile has a highly mobile, mosaic genome. Nat Genet.
457 2006;38(7):779-86.
458 33. Zhao H, Nickle DC, Zeng Z, Law PYT, Wilcox MH, et al. Global Landscape of Clostridioides
459 Difficile Phylogeography, Antibiotic Susceptibility, and Toxin Polymorphisms by Post-Hoc Whole-
460 Genome Sequencing from the MODIFY I/II Studies. Infect Dis Ther. 2021;10(2):853-70.
461 34. Seth-Smith HMB, Biggel M, Roloff T, Hinic V, Bodmer T, et al. Transition From PCR-Ribotyping
462 to Whole Genome Sequencing Based Typing of Clostridioides difficile. Front Cell Infect Microbiol.
463 2021;11:681518.
464 35. Oliveira PH, Ribis JW, Garrett EM, Trzilova D, Kim A, et al. Epigenomic characterization of
465 Clostridioides difficile finds a conserved DNA methyltransferase that mediates sporulation and
466 pathogenesis. Nat Microbiol. 2020;5(1):166-80.
467 36. van Eijk E, Anvar SY, Browne HP, Leung WY, Frank J, et al. Complete genome sequence of the
468 Clostridium difficile laboratory strain 630Δerm reveals differences from strain 630, including
469 translocation of the mobile element CTn5. BMC Genomics. 2015;16(1):31.
470 37. Imwattana K, Knight DR, Kullin B, Collins DA, Putsathit P, et al. Clostridium difficile ribotype
471 017 - characterization, evolution and epidemiology of the dominant strain in Asia. Emerg Microbes
472 Infect. 2019;8(1):796-807.
473 38. Shivaperumal N, Knight DR, Imwattana K, Androga GO, Chang BJ, et al. Esculin hydrolysis
474 negative and TcdA-only producing strains of clostridium (Clostridiodes) difficile from the
475 environment in Western Australia. J Appl Microbiol. 2022.
476 39. Turner NA, Grambow SC, Woods CW, Fowler VG, Jr., Moehring RW, et al. Epidemiologic
477 Trends in Clostridioides difficile Infections in a Regional Community Hospital Network. JAMA Netw
478 Open. 2019;2(10):e1914149.
479 40. Gilchrist CLM, Chooi Y-H. clinker & clustermap.js: automatic generation of gene cluster
480 comparison figures. Bioinformatics. 2021;37(16):2473-5.

481

SUPPLEMENTAL INFORMATION

Supplemental Table S1. Characteristics of RT151 isolates and reference sequences analyzed in this study.

PCR RT151 isolates																					
Name	**Clade**	**RT**	**RT151[1]**	**ST**	**ST205[1]**	**Accession_Illumina_reads**	**Accession_PacBio**	**Accession_Assembly**	**Sample_alias**	**Identifier**	**Reference**	**Country_Isolation**	**State_city**	**Source**	**Year_Isolation**	**Collection**	**Xpert_Cddifficile_BT**	**Toxin_neutralization_assay**	**VIDAS**	**UMC_multiplex[2]**	**UMCU_tcdB_RTPCR[3]**	**ChromID**
R181528	1		151	Yes	948	ST205-like	ERR9902328			Cdiff_RT151_1	R181528	This_study	Germany	Freiburg		2003	UK Anaerobic Reference Unit						
R182848	1		151	Yes	205	Yes	ERR9902329			Cdiff_RT151_2	R182848	This_study	USA	Arizona		2003	UK Anaerobic Reference Unit						
R201898	1		151	Yes	205	Yes	ERR9902330			Cdiff_RT151_3	R201898	This_study	USA	Arizona		2004	UK Anaerobic Reference Unit						
R542308	1		151	Yes	205	Yes	ERR9902331			Cdiff_RT151_4	R542308	This_study	Wales	Newport		2019	UK Anaerobic Reference Unit						
LUMCMM11 0004	1		151	Yes	205	Yes	ERR9902332			Cdiff_RT151_5	104875-001-011	This_study	Netherlands	Nijmegen		2011	LUMC	negative	negative	negative	11000	negative	positive
LUMCMM16 0013	C-I		151	Yes	759	No	ERR9902333	ERR9902350	GCA_945909635	Cdiff_RT151_6	104875-001-012	This_study	Netherlands	Nijmegen		2016	LUMC	negative	negative	equivalent	11000	negative	positive
LUMCMM21 0001 / LUMC-II			151	Yes	946	No	ERR9902334	ERR9902351	GCA_945901085	Cdiff_RT151_7	104875-001-013	This_study	Netherlands	Utrecht	CDI_patient	2021	LUMC	negative	weak[4]	positive[5]	11010	positive	positive
LUMCMM19 2333	C-II		151	Yes	947	No	ERR9902335	ERR9902352	GCA_945909465	Cdiff_RT151_8	104875-001-016	This_study	Malta			2019	LUMC	negative	negative	equivalent	11100	negative	positive
LUMCMM19 2334	1		151	Yes	205	Yes	ERR9902336			Cdiff_RT151_9	104875-001-017	This_study	Greece			2019	LUMC	negative	negative	equivalent	11000	negative	positive
LUMCMM16 0014	1		151	Yes	205	Yes	ERR9902337			Cdiff_RT151_10	104875-001-018	This_study	Spain		Animal	2016	LUMC	negative	negative	negative	11000	negative	positive
LUMCMM16 0015	1		151	Yes	205	Yes	ERR9902338			Cdiff_RT151_11	104875-001-019	This_study	Spain		Animal	2016	LUMC	negative	negative	equivalent	11000	negative	positive
Reference sequences																							
	C-III	Unknown	No	369	No	ERR2215081				ERR2215081	10.1128/ICM.01987-17												
	C-III	Unknown	No	343	No	ERR2216003				ERR2216003	10.1128/ICM.01987-17												
	C-II	Unknown	No	200	No	SRR3654506				SRR3654506	10.1371/journal.pone.0182307												
	C-II	Unknown	No	637	No	ERR3236451				ERR3236451	10.1038/srep43464-4												
	C-I	Unknown	No	178	No	ERR231399				ERR231399	10.1093/gbe/evz204												
	C-I	Unknown	No	314	No	SRR3629659				SRR3629659	10.1371/journal.pone.0182307												
	1	1	No	3	No	SRR1519369				001-LL-SRR1519369	10.1128/ICM.01737-21												
	1	12	No	54	No	SRR1519379				012-LL-SRR1519379	10.1128/ICM.01737-21												
	2	16	No	1	No	SRR1519382				016-LL-SRR1519382	10.1128/ICM.01737-21												
	4	17	No	37	No	SRR1519383				017-LL-SRR1519383	10.1128/ICM.01737-21												
	3	23	No	5	No	SRR1519388				023-LL-SRR1519388	10.1128/ICM.01737-21												
	1	26	No	7	No	SRR1519390				026-LL-SRR1519390	10.1128/ICM.01737-21												
	2	27	No	1	No	SRR1519391				027-LL-SRR1519391	10.1128/ICM.01737-21												
	4	40	No	121	No	SRR1519398				040-LL-SRR1519398	10.1128/ICM.01737-21												
	1	57	No	55	No	SRR1519410				057-LL-SRR1519410	10.1128/ICM.01737-21												
	3	58	No	96	No	SRR1519411				058-LL-SRR1519411	10.1128/ICM.01737-21												
	5	66	No	11	No	SRR1519416				066-LL-SRR1519416	10.1128/ICM.01737-21												
	5	78	No	11	No	SRR1519423				078-LL-SRR1519423	10.1128/ICM.01737-21												
Abbreviations: RT = PCR ribotype, ST = (7-gene multilocus) sequence type																							
[1] classifier used in Figures 1 and 2																							
[2] "weak" indicates a partial cytopathic effect, only observed with undiluted culture supernatant, on VeroC6 cells after 48h																							
[3] "positive" corresponds to a value of 0.99																							
[4] Numbers indicate positive (1) or negative (0) for 16S, *gluD*, *tcdA*, *tcdB* and *cdt* (in that order). For reference see main manuscript.																							
[5] For reference see main manuscript.																							

Supplemental Table S2. Overview of modified base motifs of the cryptic clade RT151 isolates.

LUMCMM16 0013 modified base motifs											
Motif	**Modified Position**	**Modification Type**	**% of Motifs Detected**	**# of Motifs Detected**	**# of Motifs in Genome**	**Mean QV**	**Mean Coverage**	**Partner Motif**	**Mean IPD ratio**	**Group Tag**	**Objective Score**
CAAAAA	6	m6A	99.7%	7,75	7,767	323.6	107.5		4.2	CAAAAA	2,502,921.2
CTKMAG	5	m6A	70.1%	3,785	5,398	359.9	109.2	CTKMAG	5.1	CTKMAG	989,662.4
VNCYSVNYAD	3	m4C	22.3%	1,897	8,475	61.9	111.3		1.7	VNCYSVNYAD	30,515.8
GNGGYVSCRN$_5$D	3	unknown	51.7%	118	228	60.6	115.8		1.8	GNGGYVSCRNNNNND	3,950.7
CGN$_7$TNGNGACNNANC	11	unknown	96.0%	24	25	68.6	126.3		1.8	CGNNTNGNGACNNANC	1,586.6
DN:ACTGAAGR	9	m6A	24.5%	52	212	94.2	109.8		2.2	DNNNNNNNACTGAAGR	1,227.8
GGNCGTN$_2$CNCTN$_4$T	4	unknown	100.0%	14	14	82.5	125.3		1.9	GGNCGTNNCNCTNNNNT	1,155.0
HTTATACNWN$_4$C	3	unknown	15.2%	117	769	51.9	105.7		1.6	HTTATACNWNNNNNC	1,115.4
TN$_2$CNGANCNCNCN$_2$TNA	4	unknown	95.8%	23	24	49.9	126.7		1.6	TNNCNGANCNCNCNNTNA	1,103.9
CWATTATCW	1	m4C	17.2%	93	538	50.8	109.7		1.6	CWATTATCW	972.7
GGN$_2$CGAMATT	2	unknown	78.5%	22	28	45.8	126.6		1.6	GGNNNCGAMATT	810.5
AN$_2$TCGNCTNANCNC	8	unknown	100.0%	13	13	59.0	125.0		1.6	ANNTCGNCTNANCNC	767.0
TN$_2$CGGNGGN$_2$GTA	9	unknown	86.6%	13	15	59.6	124.8		1.7	TNNNCGGNGGNNGTA	681.3
CGNCCTN$_2$CAN$_2$GC	5	m4C	100.0%	12	12	53.5	126.8		1.6	CGNCCTNNNCANNNGC	642.0
LUMCMM21 0003 modified base motifs											
Modified Base Motifs											
Motif	**Modified Position**	**Modification Type**	**% of Motifs Detected**	**# of Motifs Detected**	**# of Motifs in Genome**	**Mean QV**	**Mean Coverage**	**Partner Motif**	**Mean IPD ratio**	**Group Tag**	**Objective Score**
CAAAAA	6	m6A	98.2%	7,668	7,807	478.3	185.5		4.1	CAAAAA	3,608,910.0
VNCYGRNCRC	3	unknown	55.1%	70	127	74.3	251.6		1.6	VNCYGRNCRC	3,042.6
CAAAAAASNV	5	m6A	16.5%	102	617	148.9	185.8		2.1	CAAAAAASNV	3,006.4
HN$_3$GCVDGCNHC	5	m4C	40.5%	73	180	62.7	226.2		1.6	HNNGCVDGCNHC	2,032.4
AN$_5$CGNCTNMNCAC	8	unknown	100.0%	24	24	68.3	314.3		1.6	ANNNCGNCTNMNCAC	1,639.0
CTATTATCW	1	m4C	28.4%	84	295	58.8	179.5		1.6	CTATTATCW	1,593.6
GTCN$_3$ACANCN$_2$CG	1	unknown	100.0%	12	12	53.6	314.0		1.5	GTCNNNACANCNNNNNCG	643.0
LUMCMM19 2333 modified base motifs											
Modified Base Motifs											
Motif	**Modified Position**	**Modification Type**	**% of Motifs Detected**	**# of Motifs Detected**	**# of Motifs in Genome**	**Mean QV**	**Mean Coverage**	**Partner Motif**	**Mean IPD ratio**	**Group Tag**	**Objective Score**
CAAAAA	6	m6A	99.5%	8,244	8,285	415.2	165.7		4.0	CAAAAA	3,407,425.2
CCAAAT	5	m6A	100.0%	3,912	3,912	489.2	166.0		4.3	CCAAAT	1,913,557.0
TAGN$_6$CTG	2	m6A	100.0%	1,175	1,175	597.9	172.2	CAGNNNNNCTA	5.7	CAGNNNNNCTA/TAGNNNNNNCTG	702,564.0
CAGN$_6$CTA	2	m6A	100.0%	1,175	1,175	588.2	172.2	TAGNNNNNCTG	5.6	CAGNNNNNCTA/TAGNNNNNNCTG	691,190.0
RGAKCT	3	m6A	12.7%	554	4,36	75.7	167.9		1.9	RGAKCT	6,547.8
CAAAAAASNV	5	m6A	15.0%	98	652	142.6	167.4		2.1	CAAAAAASNV	2,537.9
CTATTATCW	1	m4C	23.4%	77	329	53.1	164.9		1.6	CTATTATCW	1,107.4
CN$_2$TNAAN$_2$GCGGC	13	unknown	100.0%	13	13	83.8	243.3		1.7	CNNNTNAANNGCGGC	1,089.0
TN$_2$TN$_2$GGCNCANCA	11	unknown	86.3%	19	22	68.2	234.8		1.6	TNNNTNNNGGCNCANCA	1,013.4

Supplemental Figure S1. Alignment of previously characterized PaLoc insertion sites for RT151 isolates in comparison with the RT012 reference strain 630[32]. **A**. Extrachromosomal element pHSJD-312. **B**. *cdu1-cdd1*. **C**. *spoVAE-cd0776*)[6]. RT151 clade 1 is LUMCMM11 0004, RT151 clade C-I is LUMCMM16 0013, and RT151 clade C-II are LUMCMM21 0001/0003 (The Netherlands) and LUMCMM19 2333 (Malta). Figure generated by clinker[40]. Colored arrows indicate similar genes; links

493 are drawn between similar genes on neighboring clusters and are shaded based on sequence

494 identity (0% white, 100% black, identity threshold for visualization 0.30).

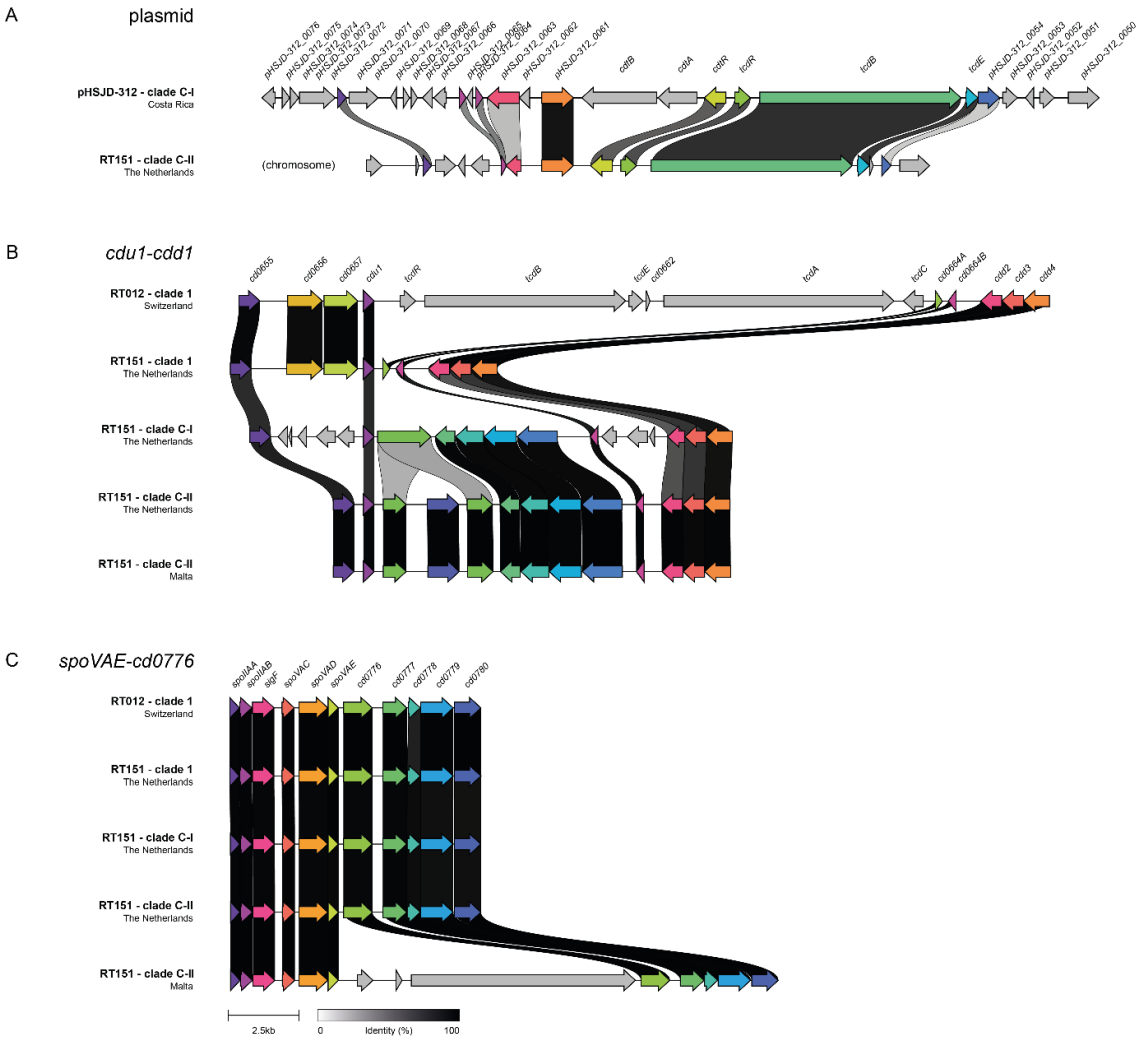

495